Water-Soluble Polymers. LXXXII. Shear Degradation Effects on Drag Reduction Behavior of Dilute Polymer Solutions

MARTIN E. COWAN, ROGER D. HESTER, CHARLES L. MCCORMICK

Department of Polymer Science, University of Southern Mississippi, Hattiesburg, Mississippi 39406

Received 27 October 2000; accepted 27 December 2000

ABSTRACT: Drag reduction measurements were conducted on extensively characterized poly(ethylene oxide) and poly(acrylamide) utilizing a fully automated rotating disk rheometer equipped with an optical tachometer, torque transducer, and software allowing real-time data acquisition. The instrument sensitivity allowed the study of concentrations as low as 0.1 ppm. In addition, previously immeasurable concentration- and time-dependent shear degradation effects were readily observed. A power law equation was shown to adequately correlate the percentage of drag reduction and the volume fraction for each polymer. Furthermore, an empirical shift factor was utilized to superimpose data from all the systems that were studied. By conducting measurements in the proper concentration and time domains, it was possible to extract the minimal concentration for the maximum drag reduction efficiency in the absence of shear degradation. The resulting values were significantly higher than those previously reported by our laboratories for poly(ethylene oxide) and poly(acrylamide). © 2001 John Wiley & Sons, Inc. J Appl Polym Sci 82: 1211–1221, 2001

Key words: water-soluble polymers; shear degradation; drag reduction

INTRODUCTION

The earliest description of the drag reduction (DR) phenomenon is attributed to Toms,[1] who observed a remarkable decrease in flow resistance of a turbulent fluid upon the addition of small amounts of polymer. Synthetic polymers,[2–5] biopolymers,[6,7] and surfactants,[8] as well as liquid suspensions of fibers and solid particles,[9] were since shown to be effective DR agents. A wide range of applications of DR can be found in processes such as crude oil transport, sewage and water line drainage, fire fighting, hydrostatic cutting, mist reduction, and marine transport.[10]

The DR phenomenon is most readily observed in dilute polymer solutions as a suppression of discrete turbulent vortices or eddies that give rise to flow inefficiency.[11] In capillary flow, three regions can be identified: a viscous boundary layer near the surface having laminar flow, a transition region, and a turbulent core.[12] The volume of the boundary layer increases with increasing polymer concentration at the expense of the turbulent core region.[13] In addition, the frequency of turbulent bursts near the boundary layer decreases with increasing polymer concentration.[14] The DR phenomenon directly correlates with decreased turbulence, but the mechanism of turbulence suppression has not been completely elucidated.

At low polymer concentrations the DR is strongly dependent on the polymer concentration (region A, Fig. 1). At some characteristic (saturated) concentration (C_{sat}) the DR becomes independent of the polymer concentration (region B, Fig.

Correspondence to: C. L. McCormick.

Contract grant sponsors: Gillette Research Institute; Department of Energy.

Journal of Applied Polymer Science, Vol. 82, 1211–1221 (2001)

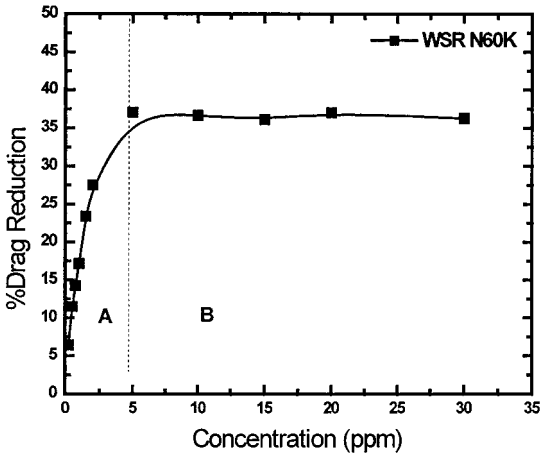

Figure 1 The percentage of drag reduction versus the polymer concentration for aqueous solutions of WSR N60K PEO (MW = 2×10^6 g/mol) as measured with a rotating disk at 1000 rpm.

1).[15] In capillary flow the C_{sat} was postulated as occurring when the buffer region expands to the center of the capillary.[15] However, this limiting geometry condition does not exist in external flow where saturated DR is also observed.[16,17]

Another explanation for saturated DR can be found in the theory of Dickerson and Hester.[18] They treated DR as a kinetic process in which polymer molecules collide with turbulent microeddies. The resulting dissipation of turbulence was thought to be the cause of the DR. In this model the turbulence energy profile in the system was assumed to be exponentially distributed with many low-energy turbulent eddies but few with high energy.[19] Turbulent eddies of lower energy, referred to as "mortal" turbulent eddies, are suppressed upon colliding with polymer coils, which results in DR. "Immortal" turbulent eddies are too energetic to be affected by collisions with polymer coils; therefore, the number of immortal turbulent eddies is thought to be independent of the polymer concentration. The number of mortal turbulent eddies present in the system is dependent on the turbulent eddy–polymer coil collision frequency, which in turn is dependent on the volume fraction occupied by each. High polymer volume fractions can effectively suppress all mortal turbulent eddies, resulting in maximum DR (DR_{max}). Beyond a concentration specific for a given polymer (C_{sat}) no further suppression of turbulence is observed, a condition referred to as saturated DR.

The measurements of DR must be conducted below C_{sat} in order to elucidate the DR mechanism(s). Virk et al. reported a universal DR equation that relates the polymer concentration to the DR at a given flow rate in a capillary flow.[13] Recasting Virk et al.'s equation, Little[20] developed the more experimentally useful eq. (1):

$$\frac{C}{\mathrm{DR}} = \frac{[C]}{\mathrm{DR}_{max}} + \frac{C}{\mathrm{DR}_{max}} \tag{1}$$

where C is the polymer concentration, DR is the percentage of DR, DR_{max} is the maximum DR, and $[C]$ is the intrinsic concentration (ppm, the concentration required to reach half DR_{max}). The $[C]$ is defined in eq. (2):

$$[C] = \frac{\mathrm{DR}_{max}}{\lim\limits_{c \to 0} \left(\dfrac{\mathrm{DR}}{C}\right)} \tag{2}$$

in which the denominator is the intrinsic DR [DR] (the DR per unit polymer concentration at infinite dilution). The percentage of DR measured with a rotating disk instrument is defined as

$$\%\ \mathrm{DR} = \frac{T_0 - T_p}{T_0} \times 100 \tag{3}$$

where T is the torque required to rotate a disk at a given rotational speed and the subscripts 0 and p represent the solvent and polymer solutions, respectively. The Little equation is limited to dilute solutions below C_{sat} (region A, Fig. 1).[20]

The Hester–Dickerson kinetic model yields eq. (4) for DR below C_{sat} as a function of polymer volume fraction

$$\frac{[\eta]C}{\mathrm{TR}} = \frac{\alpha}{\delta} + \alpha[\eta]C \tag{4}$$

in which $[\eta]C$ is the polymer volume fraction, TR is the turbulence reduction, δ is the ratio of rate constants for turbulence suppression by the polymer to that by the solvent, and α is the ratio of the total turbulence to the mortal turbulence. The concept of turbulence reduction was first introduced by Shin[21] to represent the approach from turbulent to laminar flow according to eq. (5):

$$\mathrm{TR} = \frac{T_0 - T_p}{T_0 - T_L} \tag{5}$$

where T_0 and T_p are defined according to eq. (3) and T_L is the predicted torque required to rotate a disk at a given revolutions per minute when the flow remains laminar. Polymer samples with greater values of δ are more efficient drag reducers. Even though the kinetic model is based on the polymer volume fraction, eqs. (1) and (4) are mathematically related[19] to $\delta = 1/[\eta][C]$ and $\alpha = 1/(k\mathrm{DR}_{\max})$, where k is a constant relating the percentage of DR to TR at a given rotating disk revolutions per minute.

The polymer volume fraction was also used to empirically normalize DR data for polymers of widely varying structures.[5,7,17] By selecting one polymer sample as a benchmark, a shift factor (Δ) can be employed to superimpose all volume fraction normalized DR data. The relative values of Δ can then be used to rank the DR efficiency (DRE) under specified conditions.

Obtaining accurate DR data is often complicated by shear degradation of the polymer chains.[17,22–29] The rate of shear degradation is greatest for high molecular weight polymers at low concentration.[27–29] Shear degradation typically results in a rapid decrease in molecular weight that approaches a limiting polymer molecular weight ($M_{t\infty}$) after long degradation times. To better understand DR mechanism(s), accurate DR data must be obtained at low polymer concentration (below C_{sat}), the concentration region where DR measurements are most susceptible to shear degradation effects.

In capillary flow experiments shear degradation occurs primarily at the capillary entrance prior to DR measurement.[25] Distinguishing shear degradation inherent to the DR process from shear degradation occurring at the capillary entrance has proved difficult. Usually, the extent of DR in the absence of shear degradation is estimated from multiple pass experiments by extrapolating data to zero passes.[30] Rotating disk instruments offer unique advantages over capillary instruments for measuring DR while minimizing shear degradation, primarily because of the absence of entrance effects and the ability to measure torque prior to appreciable shear degradation (near time zero).

In this article we report DR studies of aqueous poly(ethylene oxide) (PEO) and poly(acrylamide) (PAAm) solutions measured with a rotating disk instrument under conditions minimizing the effects of shear degradation. The DR measurements were performed for polymer concentrations as low as 0.1 ppm (w/w) and analyzed using the Little eq. (1) and kinetic model eq. (4). A power law relationship between the DR and polymer concentration was successfully determined for each polymer that was examined. In addition, a concentration-dependent onset of shear degradation was measured.

EXPERIMENTAL

Materials

The AAm and potassium persulfate were purchased from Aldrich and recrystallized twice from acetone and deionized water, respectively. The PAAm was synthesized by the solution polymerization of 0.5*M* AAm solution in deionized water at 30°C with 0.1% (w/w) potassium persulfate as the initiator as described previously.[31] The polymerization was terminated by precipitation into acetone. The polymer product was redissolved in deionized water and dialyzed against deionized water using Spectra/Por 4 dialysis bags with molecular weight cutoffs of 12,000–14,000 Da. The PEO samples with reported viscosity-average molecular weights of 0.9×10^6, 2×10^6, and 4×10^6 were supplied by Union Carbide. Stock solutions were prepared in deionized water (18.2 MΩ resistivity) and allowed to age for 1 month with sodium azide added at a concentration of 0.01% (w/w) as a biocide.

Characterization

Viscometry

Low shear intrinsic viscosity measurements were performed using a Contraves LS30 low shear viscometer at a shear rate of 5.9/s. The intrinsic viscosity measurements were determined using the Huggins and Kraemer equations.

Light Scattering

The refractive index increments (dn/dc) were determined using a Chromatix KMX-16 laser differential refractometer. Polymer solutions were clarified with 1-mm Millipore filters. The polymer concentration was determined before and after filtration by UV spectroscopy to confirm that no polymer was lost during the filtration process. Classical light scattering measurements were performed at 25°C using a Brookhaven Instruments BI-200SM automatic goniometer interfaced with a personal computer. Excess scattered

Table I Nomenclature and Physical Parameters of Polymer Samples

Polymer	$[\eta]$ (dL/g)	M_w (g/mol)
PAAm	15.2	2.0×10^6
WSR 301 PEO	18.6	4.3×10^6
WSR N60K PEO	10.1	2.0×10^6
WSR 1105 PEO	5.5	0.55×10^6

$[\eta]$, the zero shear intrinsic viscosity values determined using low shear rheometry; M_w, the weight-average molecular weight measured by multiangle laser light scattering.

intensity measurements were obtained at multiple angles between 30 and 150°. Zimm plots were generated using software provided by the manufacturer.

DR Measurements

The DR measurements in this study were performed using a rotating disk rheometer designed in our laboratories. The rheometer consists of an 18.5-L cylindrical tank (30.5-cm o.d., 0.953-cm wall thickness) with a removable polycarbonate cover. A 9.0-cm radius stainless steel disk and spindle assembly driven by a Maxon 80-W dc motor generated the rotational flow field. The spindle assembly rests in a bushing at the bottom of the sample vessel to stabilize the disk during rotation. An HP HEDS-6310 optical tachometer and a Vibrac TQ-100 torque transducer constantly measure the instrument performance while a computer utilizing National Instrument's LabView® software controls the rotational speed of the disk.

Stock solutions of 5000 ppm (w/w) were prepared for each polymer sample and were allowed to age for at least 1 month with 0.01 wt % sodium azide added as a biocide. The proper amount of stock solution was diluted in the rotating disk instrument reservoir to give the desired concentration for each DR experiment. The percentage of DR (%DR) and TR are defined in eqs. (3) and (5) above. As stated previously, the T_{polymer} increased with time due to shear degradation. To minimize this effect, only T_{polymer} values measured within 10 s of equilibration were used to calculate %DR and TR. The DR data were found to be reproducible to within ±2%.

RESULTS AND DISCUSSION

The purpose of this work was to examine the relationship between the polymer concentration and DR at a constant Reynolds number in a rotating disk system by measuring the DR below C_{sat} under conditions minimizing shear degradation. Several DR models from the literature were employed to compare the DRE of the polymers examined in this study. In addition, the concentration-dependent shear degradation behavior was examined.

Polymers Utilized in Study

Three PEO samples of different molecular weights (WSR 1105, N60K, and 301) and one PAAm sample were selected for this study. The molecular weights and dilute solution viscosity data can be found in Table I. The weight-average molecular weight values as determined by classical light scattering ranged from (0.55 to 4.3) $\times 10^6$ g/mol.

DR Measurements

The DR curves for all four samples as a function of the concentration are shown in Figures 2 and 3. The DR effectiveness of aqueous PEO solutions increased with increasing molecular weight,[32] resulting in an inverse relationship between the values of C_{sat} and the molecular weight. The C_{sat} value for WSR 1105 PEO was estimated from Figure 2 to be near 50 ppm (w/w), while the C_{sat} values for WSR 301 PEO, PAAm, and WSR N60K

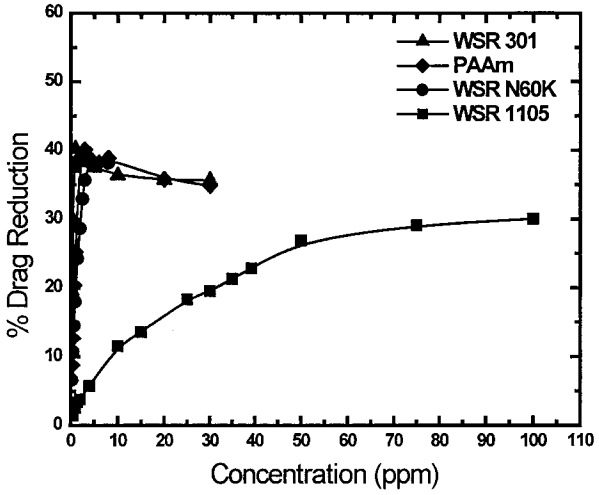

Figure 2 The percentage of drag reduction measured with a rotating disk at 1000 rpm versus the polymer concentration for aqueous solutions of PAAm and PEO samples with molecular weights ranging from (0.55 to 4.3) $\times 10^6$ g/mol.

PEO were estimated from Figure 3 to be 0.75, 2, and 3 ppm (w/w), respectively. These values were lower than values reported from previous DR studies.[16,20,33]

DR Data Analyzed by Little Equation

The concentration-dependent DR behavior can be examined by using the relationship of Little. Plotting C/DR versus C (Fig. 4) from eq. (1) allowed the determination of the DR_{max}, [C], and [DR]. Efficient drag reducers exhibit large values of [DR] and low values of [C]. Application of this relationship is restricted to low concentrations[20]; therefore, only DR data below C_{sat} were used in this analysis.

Compound WSR 301 PEO was the most efficient drag-reducing polymer in this study with values of 92.7 ppm^{-1} and 0.98 ppm for the [DR] and [C], respectively (Table II). The WSR N60K PEO and PAAm samples had comparable [DR] values; however, the [C] value for the PAAm sample was twice that of WSR N60K PEO. The poorest drag-reducing polymer in the study based on concentration was WSR 1105 PEO.

The slope values for the lines representing WSR 301 PEO and PAAm (Fig. 4) had lower than expected DR_{max} values of 91.0 and 96.5%, respectively (Table II). Within the PEO series a linear relationship was observed for the $[C]^{-1}$ and molecular weight (Fig. 5), predicting a lower molecular weight limit of 1.5×10^5 g/mol (x intercept), below which no DR was expected. This corresponded well with the molecular weight limit of 1.1×10^5 g/mol reported by Little[20] for DR of aqueous PEO solutions in capillary flow, but it contrasted with a previous prediction of no lower molecular weight limit for DR measured with a rotating disk instrument.[16]

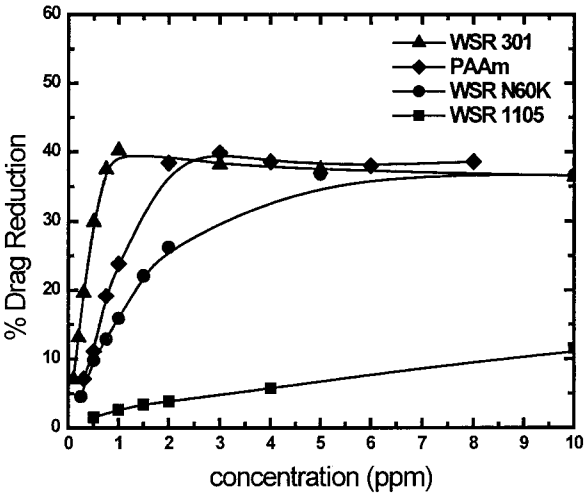

Figure 3 The percentage of drag reduction measured with a rotating disk at 1000 rpm versus the polymer concentration for aqueous solutions of PAAm and PEO samples with molecular weights ranging from (0.55 to 4.3) $\times 10^6$ g/mol.

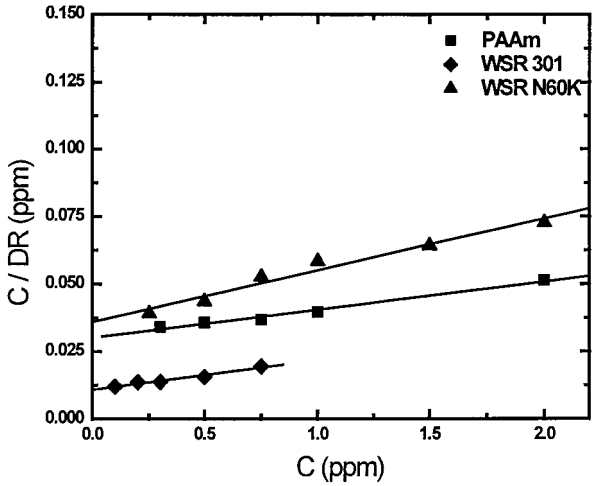

Figure 4 The drag reduction data measured with a rotating disk at 1000 rpm plotted according to eq. (1). The drag reduction data for WSR 1105 PEO are not shown because of differences in scale.

DR Data Analyzed by Kinetic Equation

The relationship between the DR and polymer volume fraction (Fig. 6) was also examined using eq. (4), which was derived from the kinetic model of Dickerson and Hester.[18] More efficient drag-reducing polymers had greater δ values (Table III). Sample WSR 301 PEO was the most efficient drag-reducing polymer based on the volume fraction, but it was only slightly greater than WSR N60K PEO. By comparison, PAAm and WSR 1105 PEO performed poorly on a volume fraction basis. Once again, the α for WSR 301 and PAAm were much lower than expected based on previously reported values.[19] Values that are greater than or equal to one are expected for highly efficient DR polymers, but the α values much less than one, as determined in the current study, are not consistent with the theory used to develop the kinetic model.

Molecular aggregates from a dilution of concentrated stock solutions were initially suspected to be responsible for the unexpectedly high DRE. A

Table II Drag Reduction Parameters as Determined from Little Equation, Eq. (1)

Polymer	DR_{max} (%)	[*C*] (ppm)	[DR] (%/ppm)	Correlation Coefficient
PAAm	96.5	2.9	33.2	0.992
WSR 301 PEO	91.0	0.98	92.7	0.981
WSR N60K PEO	52.3	1.9	27.8	0.984
WSR 1105 PEO	29.9	14.7	2.0	0.985

DR_{max}, the theoretical maximum percent drag reduction; [*C*], the intrinsic concentration, which is the concentration required to achieve one-half DR_{max}; [DR], the intrinsic drag reduction, which is the predicted percent drag reduction per parts per million of polymer at infinite dilution.

study was conducted in which low revolutions per minute mixing of diluted stock solutions was performed for times ranging from 0 to 24 h (Fig. 7) prior to DR measurements. In addition, a stock solution was prepared at the same concentration to be used in the DR experiment and allowed to age for 1 month with occasional gentle stirring. No differences were observed for any of the torque measurements (within experimental error), regardless of mixing time or stock solution concentration, which strongly suggested that molecular aggregation was not responsible for the better than anticipated DR results.

Volume Fraction Normalization

McCormick et al.'s[5,7,17] series of publications explored the role of the polymer volume fraction in DR for a variety of well-characterized synthetic poly(acrylamido) polymers. The volume fraction, as estimated by the product of the intrinsic viscosity and concentration, was utilized to account for polymer molecular weight and polymer–solvent interaction. This treatment yielded curves of similar shape, and a shift factor Δ was employed to normalize the DR data to a single, universal curve, regardless of the polymer type or molecular weight. The Δ provided a relative measure of the DRE. Figure 8 is a plot of the DR normalized by the polymer volume fraction plotted versus the volume fraction. As can be seen, curves of similar shape exist for the PEO and PAAm polymers examined in this study. Selecting PAAm as the benchmark polymer, a Δ was utilized to superimpose the DR data of the PEO samples onto the PAAm data. The shifted data along with the Δ values can be seen in Figure 9. Values of Δ greater

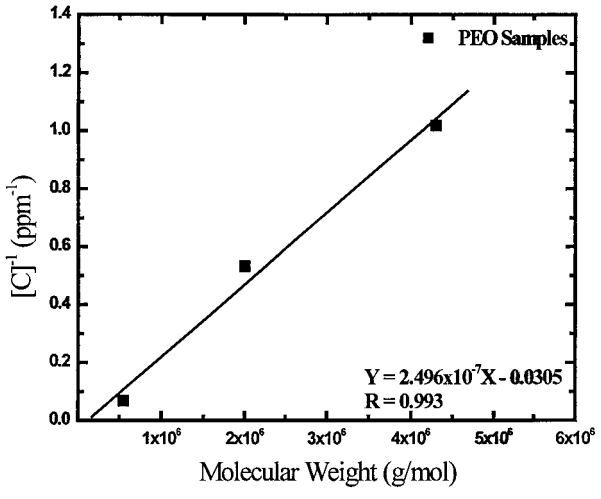

Figure 5 The inverse intrinsic concentration ([*C*] − 1) versus the molecular weight for aqueous solutions of PEO measured with a rotating disk at 1000 rpm.

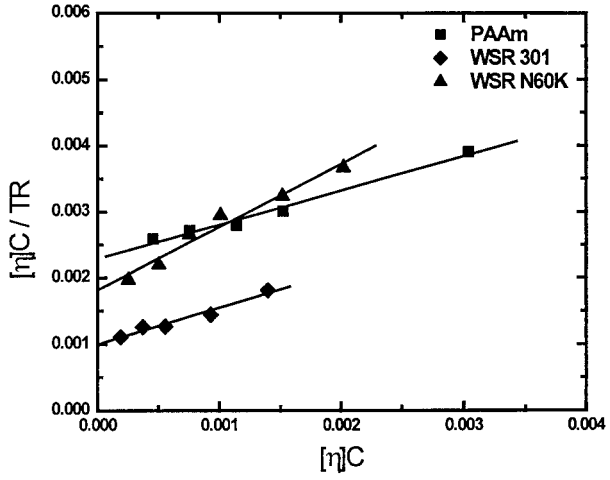

Figure 6 The drag reduction data measured with a rotating disk at 1000 rpm plotted according to eq. (4). The drag reduction data for WSR 1105 PEO are not shown because of differences in scale.

Table III Drag Reduction Parameters as Determined from Dickerson–Hester Kinetic Model

Polymer	α	TR_{max} (%)	δ
PAAm	0.518	193	226
WSR 301 PEO	0.550	181	549
WSR N60K PEO	0.955	105	524
WSR 1105 PEO	1.67	59.7	124

α, the volume fraction ratio of total turbulence to mortal turbulence; TR_{max}, the theoretical maximum percent turbulence reduction; δ, the ratio of rate constants for turbulence suppression by the polymer to that by the solvent.

than 1.0 indicate more efficient DR on a volume fraction basis, while Δ values less than one indicate less efficient DR. Not unexpectedly, WSR 301 PEO was the most efficient drag-reducing polymer based on the volume fraction in this study with a Δ value of 2.3. Samples WSR N60K PEO and PAAm behaved similarly with Δ values near one, despite behaving differently on a concentration basis (Fig. 4). Once again, WSR 1105 PEO was the poorest drag-reducing polymer in this study with a Δ value of 0.1.

Volume Fraction Dependent DR

The data acquired in this study below C_{sat} under experimental conditions and minimizing shear degradation were ideal for examining the relationship between the $[\eta]C$ and the DR. Linear, power, logarithmic, and exponential relationships were used to empirically describe the volume fraction dependence on the DR. A power law equation of the form

$$\% \text{ DR} = A_{[\eta]C}([\eta]C)^B \quad (6)$$

where $A_{[\eta]C}$ and B are constants, gives the best average correlation coefficient value (0.992). The

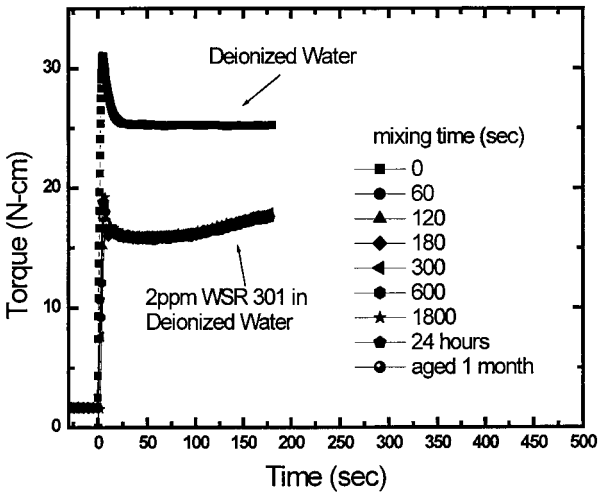

Figure 7 The torque required to maintain 1000 rpm versus the time for 2-ppm polymer solutions. The solutions were prepared by diluting a 5000-ppm stock solution and mixing at 300 rpm for times ranging from 0 to 24 h. Also shown is the torque versus time data for a 2-ppm stock solution aged 1 month prior to torque measurement.

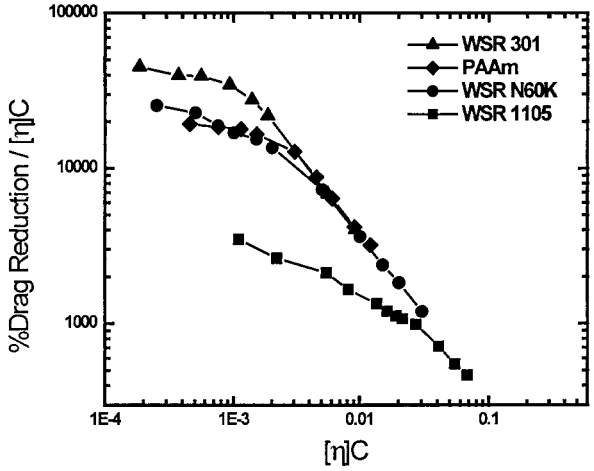

Figure 8 The drag reduction data for aqueous solutions of PAAm and PEO samples measured with a rotating disk at 1000 rpm as normalized for polymer volume fraction versus polymer volume fraction.

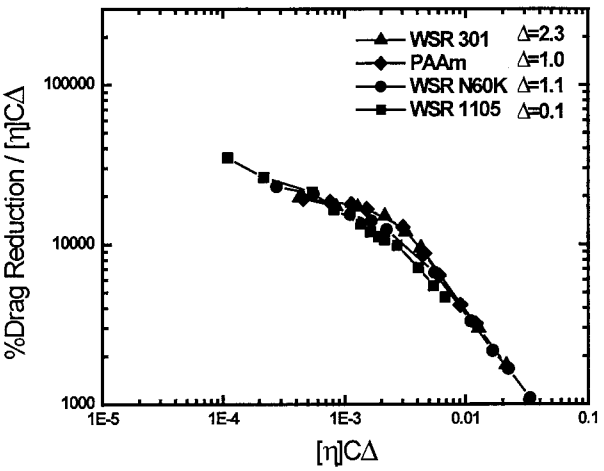

Figure 9 The drag reduction data for aqueous solutions of PAAm and PEO samples measured with a rotating disk at 1000 rpm as normalized for polymer volume fraction versus polymer volume fraction shifted by Δ to superimpose the PAAm data.

Table IV Power Law Parameters from Regression of Drag Reduction Data to Volume Fraction According to Eq. (7)

Polymer	$A_{[\eta]C}$	B	Correlation Coefficient
PAAm	3990	0.79	0.995
WSR 301 PEO	6940	0.78	0.995
WSR N60K PEO	2070	0.69	0.998
WSR 1105 PEO	305	0.66	0.996

B constant and the correlation coefficients from the fit of the DR data utilizing eq. (6) are shown in Table IV. The data are plotted in log space according to eq. (6) in Figure 10.

Multiplying the abscissa values in Figure 10 by the previously calculated Δ values resulted in the superimposition of the DR data for the PEO and PAAm samples examined in this study (Fig. 11). Plotted in this manner, a slope difference in the DR data for the different polymer samples was evident that could not be accounted for by the Δ value alone. This implied a subtle difference in DR behavior with a changing polymer volume fraction for the different polymer samples (also seen in Fig. 9).

Shear Degradation

The DR behavior was greatly affected by polymer shear degradation as illustrated in Figure 7. In a rotating disk experiment a constant rotational velocity is maintained while torque is measured. Upon reaching equilibrium (t = 30 s), the torque values for the solvent remain constant while the torque values for the polymer solutions increase with time because of shear degradation of the polymer chains. To better quantify the effect of polymer shear degradation on the DR, torque as a function of time was measured with the rotating disk system for aqueous solutions of WSR 301 PEO (Fig. 12). Time zero was defined as the time

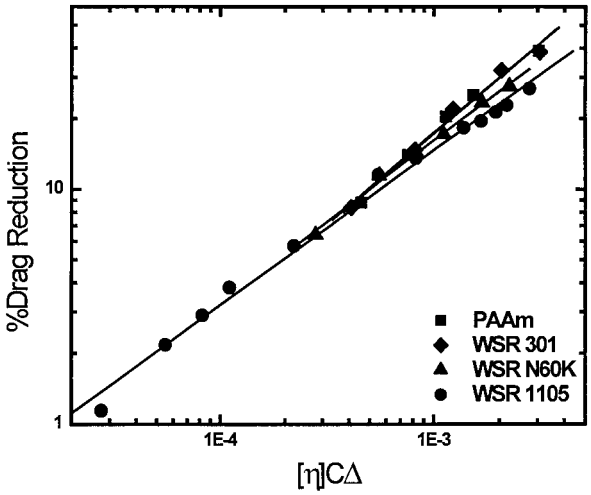

Figure 11 The drag reduction data for aqueous solutions of PAAm and PEO samples measured with a rotating disk at 1000 rpm versus the polymer volume fraction $[\eta]C$ multiplied by the DRE factor Δ.

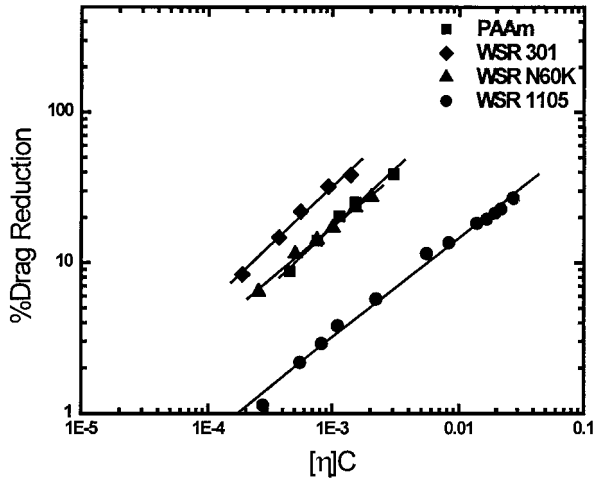

Figure 10 The drag reduction data for aqueous solutions of PAAm and PEO samples measured with a rotating disk at 1000 rpm versus the polymer volume fraction $[\eta]C$.

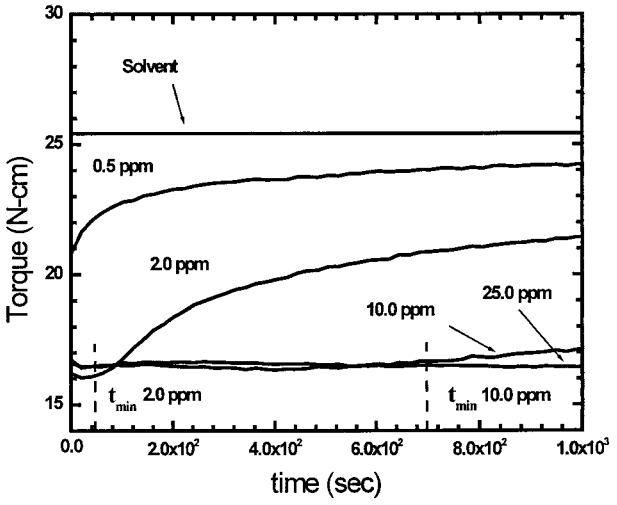

Figure 12 The torque required to maintain a rotational velocity of 1000 rpm the versus time for aqueous solutions of WSR 301 PEO of varying concentrations.

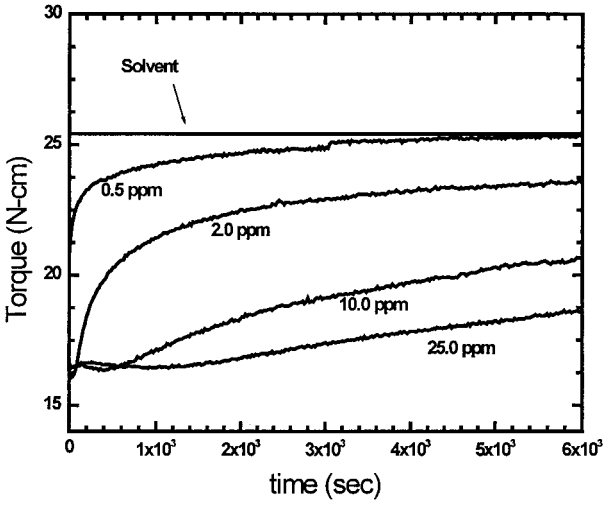

Figure 13 The torque required to maintain a rotational velocity of 1000 rpm versus the time for aqueous solutions of WSR 301 PEO of varying concentrations. The time was recorded when equilibrium was attained (approximately 30 s).

when the torque value for the solvent reaches equilibrium. Solution concentrations of 0.5, 2, 10, and 25 ppm (w/w) were selected to examine the effects of shear degradation on DR as a function of the polymer concentration above and below C_{sat}.

Different torque responses with time were observed for polymer concentrations above and below C_{sat}. Below C_{sat} (0.5-ppm solution) the torque value immediately began to increase as time progressed. Above C_{sat} a common torque minimum (approximately 16.6 N cm) was observed, regardless of the polymer concentration (2, 10, or 25 ppm), and was maintained for a length of time (t_{min}). Values for t_{min} of 45, 700, and 1800 s were measured for WSR 301 PEO concentrations of 2, 10, and 25 ppm, respectively (Figs. 12, 13). A plot of t_{min} versus the polymer concentration (Fig. 14) yielded a linear relationship with the slope, y intercept, and correlation coefficient values of 75.9, −88.1, and 0.999, respectively. A C_{sat} value of 1.2 ppm was determined for WSR 301 PEO in deionized water from the x intercept in Figure 14.

The Dickerson–Hester model can be used to explain the origin of t_{min} in rotating disk instruments. At high rotational disk speeds, turbulent flow is established near the disk surface by the continuous generation of turbulent eddies that diffuse away from the disk where they are dissipated by fluid viscous forces. The turbulent eddies near the disk create increased fluid drag. Dissolved polymer coils interact with and suppress mortal turbulent eddies, resulting in a decrease in the equilibrium number of turbulent eddies near the disk and giving rise to DR. Above C_{sat} the number of effective drag-reducing polymer coils is great enough to suppress all mortal turbulent eddies. With time, however, the number of effective drag-reducing polymer coils decreases because of shear degradation. At time t_{min} the DRE of the system begins to diminish because the number of coils is insufficient to suppress all mortal turbulent eddies. Therefore, at times greater than t_{min}, increasing torque values are observed.

The shear degradation rate, as represented by the slope of torque versus time data after t_{min}, decreased with increasing polymer concentration (Figs. 12, 14). This concentration-dependent degradation rate can be better understood by examining data acquired at extended times. In Figure 15 the torque values measured for aqueous solutions of WSR 301 PEO are plotted versus time. Within 24 h shear degradation was no longer observed, but the asymptotic torque values reached at long times were less than for solvent alone and decreased in magnitude with increasing polymer concentration.

Figure 15 suggests that under the current experimental conditions, higher molecular weight polymer molecules were continually being degraded by fluid turbulence into chains of lower molecular weight as time progressed. These lower molecular weight polymers were less effective at reducing drag and therefore the torque steadily increased with time. For any polymer concentra-

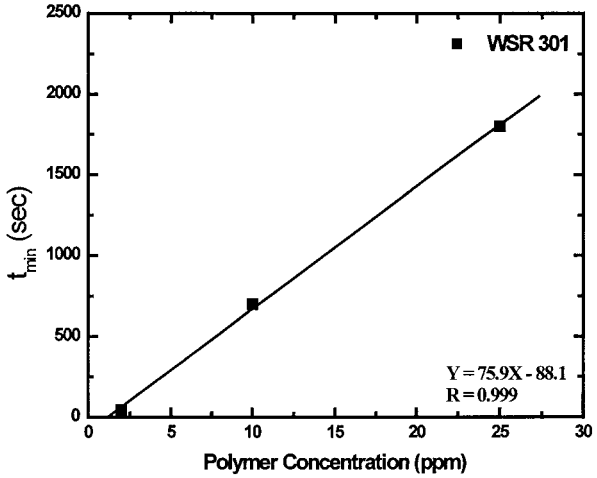

Figure 14 The time required for shear degradation to impact the drag reduction (t_{min}) versus the polymer concentration for aqueous solutions of WSR 301 PEO as measured with a rotating disk instrument at 1000 rpm.

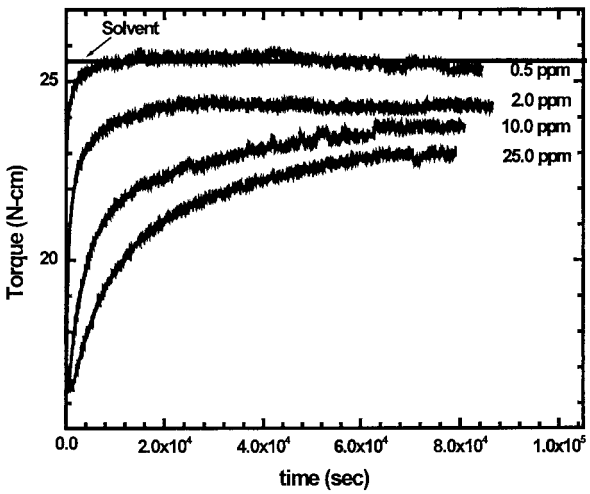

Figure 15 The torque required to maintain a rotational velocity of 1000 rpm versus the time for aqueous solutions of WSR 301 PEO of varying concentration weights ranging from (0.55 to 4.3) $\times$ 10^6 g/mol.

tion at time zero, no polymer underwent degradation and the rate of degradation would be a maximum. However, as time progressed less polymer of higher molecular weight existed and thus the rate of degradation decreased because less polymer was available for degradation. This was reflected as a decrease in the rate at which the torque increased. Eventually, all the polymer that could be degraded was degraded and the rate of degradation approached zero. At this time a steady-state polymer molecular weight was reached and the torque stabilized to some constant value. Because the final solution torque value was less than the solvent torque value, it was concluded that the low molecular weight polymer chains produced by extended degradation in our rotating disk apparatus were still capable of reducing drag but to a lesser degree than the undegraded polymer. The final torque value was inversely related to the amount of low molecular weight polymer present; thus, the higher polymer concentration solutions had the lower torque values. This result was in contrast to the findings of Hunston and Zakin who studied the DR behavior of polystyrene in toluene.[28] Apparently in that study the low molecular weight polystyrene molecules produced by degradation in their apparatus did not have DR capability.

CONCLUSIONS

A rotating disk apparatus designed in our laboratories was used to perform DR measurements on several well-characterized, high molecular weight, water-soluble polymers. Polymer concentrations as low as 0.1 ppm were studied under experimental conditions largely negating the effects of shear degradation. The values for C_{sat}, the polymer concentration required to reach saturated DR, were nearly an order of magnitude less than those previously reported for the same polymer–solvent systems of similar molecular weights. Polymer aggregation was ruled out as being the cause of the increased DRE. We attributed the discrepancy to previously immeasurable shear degradation effects. A power law equation was found to adequately fit all DR data below C_{sat} to the volume fraction. The shift factor Δ successfully superimposesd all of the data; however, slight differences in slope were observed for each of the samples.

Financial support from the Gillette Research Institute and the Department of Energy is gratefully acknowledged. Jim Slemp of Radical Systems, Huntsville, AL, and Steve Selph of the University of Southern Mississippi are greatly appreciated for assisting with the data acquisition and control system.

REFERENCES

1. Toms, B. A. In First International Congress on Rheology, 1948; Amsterdam: North Holland, 1948.
2. Sellin, R. H. J.; Hoyt, J. W.; Pollert, J.; Scrivener, O. J Hydraul Res 1982, 20, 235.
3. Sellin, R. H. J.; Hoyt, J. W.; Scrivener, O. J Hydraul Res 1982, 20, 29.
4. McCormick, C. L.; Hester, R. D.; Morgan, S. E.; Safieddine, A. M. Macromolecules 1990, 23, 2132.
5. McCormick, C. L.; Hester, R. D.; Morgan, S. E.; Safieddine, A. M. Macromolecules 1990, 23, 2124.
6. Hoyt, J. W. Trends Biotechnol 1985, 3, 17.
7. Morgan, S. E.; McCormick, C. L. Prog Polym Sci 1990, 15, 507.
8. Shenoy, A. V. Colloid Polym Sci 1984, 262, 455.
9. Metzner, A. B.; Kale, D. D. AIChE J 1976, 22, 669.
10. Kulicke, W.-M.; Kotter, M.; Grager, H. Advances in Polymer Science; Springer–Verlag: Berlin, 1989; p 1.
11. Davies, J. T. Turbulence Phenomena; Academic: New York, 1972.
12. Lumley, J. L.; Kubo, I. In The Influence of Polymer Additives on the Velocity and Temperature Fields; Gampert, B., Ed.; Springer–Verlag: Berlin, 1984; p 3.
13. Virk, P. S.; Merrill, E. W.; Mickley, H. S.; Smith, K. A.; Mollo-Christensen, E. L. J Fluid Mech 1967, 30, 305.

14. Donohue, G. L.; Tiederman, W. G.; Reischman, M. M. J Fluid Mech 1972, 56, 559.
15. Virk, P. S. In Biotechnology of Marine Polysaccharides; Colwell, R., Pariser, E. R., Sinsky, A. J., Eds.; Hemisphere: Washington, DC, 1985; p 149.
16. Little, R. C.; Patterson, R. L.; Ting, R. Y. J Chem Eng Data 1976, 21, 281.
17. Mumick, P. S.; Welch, P. M.; Salazar, L. C.; McCormick, C. L. Macromolecules 1994, 27, 323.
18. Dickerson, J. P.; Hester, R. D. Polym Prepr ACS Div Polym Chem 1992, 33, 317.
19. Dickerson, J. P. Ph.D. Thesis, University of Southern Mississippi, 1993.
20. Little, R. C. J Colloid Interface Sci 1971, 37, 811.
21. Shin, H. Ph.D. Thesis, Massachusetts Institute of Technology, 1965.
22. Culter, J. D.; Zakin, J. L.; Patterson, G. K. J Appl Polym Sci 1975, 19, 3235.
23. Gampert, B.; Wagner, P. In The Influence of Polymer Additives on the Velocity and Temperature Fields; Gampert, B., Ed.; Springer–Verlag: New York, 1985; p 71.
24. Patterson, R. W.; Abernathy, F. H. J Fluid Mech 1970, 43, 689.
25. Moussa, T.; Tiu, C. Chem Eng Sci 1994, 49, 1681.
26. Ram, A.; Kadim, A. J Appl Polym Sci 1970, 14, 2145.
27. Hunston, D. L. J Polym Sci Polym Chem Ed 1976, 14, 713.
28. Hunston, D. L.; Zakin, J. L. Polym Eng Sci 1980, 20, 517.
29. Zakin, J. L.; Hunston, D. L. J Macromol Sci Phys 1980, B18, 795.
30. Gramain, P.; Borreill, J. Rheol Acta 1978, 17, 303.
31. McCormick, C. L.; Blackmon, K. P. Macromolecules 1986, 19, 1512.
32. Pruitt, G. T.; Crawford, H. R. Report DTMB; Western Co.: 1965.
33. Mumick, P. S. Ph.D. Thesis, University of Southern Mississippi, 1993; p 196.